Molecular Neurobiology (2019) 56:5987–5997
https://doi.org/10.1007/s12035-019-1499-0

Inhibition of Semaphorin3A Promotes Ocular Dominance Plasticity in the Adult Rat Visual Cortex

Elena Maria Boggio[1] · Erich M. Ehlert[2] · Leonardo Lupori[3] · Elizabeth B. Moloney[2] · Fred De Winter[2] · Craig W. Vander Kooi[4] · Laura Baroncelli[1,5] · Vasilis Mecollari[2] · Bas Blits[6] · James W. Fawcett[7] · Joost Verhaagen[2,8] · Tommaso Pizzorusso[1,3,9]

Received: 11 May 2018 / Accepted: 17 January 2019 / Published online: 31 January 2019

Abstract

Perineuronal nets (PNNs) are condensed structures in the extracellular matrix that mainly surround GABA-ergic parvalbumin-positive interneurons in the adult brain. Previous studies revealed a parallel between PNN formation and the closure of the critical period. Moreover, ocular dominance plasticity is enhanced in response to PNN manipulations in adult animals. However, the mechanisms through which perineuronal nets modulate plasticity are still poorly understood. Recent work indicated that perineuronal nets may convey molecular signals by binding and storing proteins with important roles in cellular communication. Here we report that semaphorin3A (Sema3A), a chemorepulsive axon guidance cue known to bind to important perineuronal net components, is necessary to dampen ocular dominance plasticity in adult rats. First, we showed that the accumulation of Sema3A in PNNs in the visual cortex correlates with critical period closure, following the same time course of perineuronal nets maturation. Second, the accumulation of Sema3A in perineuronal nets was significantly reduced by rearing animals in the dark in the absence of any visual experience. Finally, we developed and characterized a tool to interfere with Sema3A signaling by means of AAV-mediated expression of receptor bodies, soluble proteins formed by the extracellular domain of the endogenous Sema3A receptor (neuropilin1) fused to a human IgG Fc fragment. By using this tool to antagonize Sema3A signaling in the adult rat visual cortex, we found that the specific inhibition of Sema3A promoted ocular dominance plasticity. Thus, Sema3A accumulates in perineuronal nets in an experience-dependent manner and its presence in the mature visual cortex inhibits plasticity.

Keywords Visual cortex · Critical period · Chondroitin sulfate · Inhibition

Elena Maria Boggio, Erich M. Ehlert, Leonardo Lupori and Elizabeth B. Moloney contributed equally to this work.

✉ Tommaso Pizzorusso
tommaso.pizzorusso@in.cnr.it

[1] Institute of Neuroscience, National Research Council CNR, Via Moruzzi, 1, 56124 Pisa, Italy

[2] Laboratory for Regeneration of Sensorimotor Systems, Netherlands Institute for Neuroscience, an Institute of the Royal Netherlands Academy of Arts and Science, Meibergdreef 47, 1105 BA Amsterdam, The Netherlands

[3] BIO@SNS lab, Scuola Normale Superiore via Moruzzi, 1, 56124 Pisa, Italy

[4] Department of Molecular and Cellular Biochemistry and Center for Structural Biology, University of Kentucky, Lexington, KY 40536, USA

[5] Department of Developmental Neuroscience, IRCCS Stella Maris Foundation, 56128 Pisa, Italy

[6] UniQure, Meibergdreef 61, 1105 BA Amsterdam, The Netherlands

[7] John van Geest Centre for Brain Repair, Robinson Way, Cambridge CB2 0PY, UK

[8] Center for Neurogenomics and Cognitive Research, Vrije Universiteit Amsterdam, De Boelelaan 20 1085, 1081 HV Amsterdam, The Netherlands

[9] Department of Neuroscience, Psychology, Drug Research and Child Health NEUROFARBA University of Florence, Area San Salvi – Pad. 26, 50135 Florence, Italy

Introduction

Perineuronal nets (PNNs) are condensed structures of extracellular matrix (ECM) that ensheath the soma, proximal axon, and dendrites of neurons in many parts of the central nervous system (CNS) [1–4]. Their maturation in the visual cortex closely matches the closure of the critical period [1, 5]. Importantly, degradation of PNNs with chondroitinase ABC (chABC) has been shown to restore a juvenile-like condition in many experimental paradigms of neuroplasticity in both mice and rats, including ocular dominance (OD) plasticity, and extinction of fear memories, thus establishing a causal connection between PNNs and reduced plasticity [1, 6–9]. Moreover, experimental paradigms known to modulate the level of plasticity in the brain (dark rearing (DR) and environmental enrichment) have also a profound impact in PNNs regulation, reinforcing the idea that plasticity and PNNs are tightly coupled [1, 10–13]. The precise molecular mechanisms that are responsible for PNNs effect on plasticity remain elusive. The great majority of the PNNs in the visual cortex of rats and mice surround parvalbumin (PV) positive neurons [1, 14], a class of inhibitory interneurons important for OD plasticity [15–23]. A proposed model suggests that the complex structures of PNNs may act as a scaffold by binding plasticity-regulating molecules and by presenting them in high concentration to the neurons they enfold [24]. Indeed, Otx2 has been shown to bind to chondroitin sulfate chains, an abundant glycosaminoglycan (GAG) in PNNs. This binding is necessary for Otx2 internalization in PV positive, PNN-bearing, interneurons and, in turn, for critical period closure [6, 25]. The PNN-binding capability of Otx2 is dependent upon a basic motif enriched in arginine-lysine (RK) doublets at its N-terminus [26]. Recent work provided evidence that semaphorin3A (Sema3A), a chemorepulsive protein prominently expressed in the postnatal and adult brain, has a strong affinity for CSPGs, is concentrated in PNNs and, like Otx2, contains an arginine-lysine rich basic domain at its C-terminus [27–29]. Moreover, enzymatic or genetic disruption of PNNs integrity leads to a decline in Sema3A-positive PNNs further confirming their binding. Within the PNN, Sema3A interacts specifically with 4,6-disulfated form of chondroitin sulfate chains (CS-E), a specific sulfation pattern in CS molecules [28, 30]. The biological effect of Sema3A binding to PNNs is still poorly understood; however, in dorsal root ganglia neurons, Sema3A is known to induce growth cone collapse and neurite growth inhibition and this effect is amplified by its binding to GAGs [27]. These results suggest that Sema3A might act as a plasticity inhibiting factor, through its accumulation in PNNs.

To test this hypothesis, we interfered with Sema3A function using secreted decoy Sema3A receptors ("receptor bodies") composed of the extracellular domain of the Sema3A receptor Neuropilin1 (Npn1) fused to human IgGFc. Npn1 is a co-receptor for Sema3A and VEGF. Therefore, two mutant isoforms of Npn1, which selectively bind to Sema3A [31] or VEGF [32], were used to discriminate between the effects of interfering with the function of Sema3A or VEGF. Adeno-associated viral vector-mediated delivery of the receptor body scavenging Sema3A, but not VEGF, promoted OD plasticity in the adult rat visual cortex indicating that persistent Sema3A signaling in the visual cortex is necessary to maintain reduced levels of plasticity.

Experimental Procedures

Animal Housing

Animals were maintained at 22 °C in 12-h light–dark cycle. For dark rearing experiments, animals were reared in complete darkness from birth. Food and water were available ad libitum. All necessary efforts were made to minimize both stress and the number of animals used. A total of 62 rats were used. All experiments were carried out in accordance with the European Communities Council Directive of November 24, 1986 (86/609/EEC) and were approved by the Italian Ministry of Health (authorization number 1152/2016-PR).

Preparation of Sema3A- or Npn-Conditioned Medium and Western Blot Analysis

HEK293T cells were transfected with Npn1-Fc, Npn1-VEGF-Fc, Npn1-Y297A-Fc, Npn1-T316R-Fc, Npn2-Fc, or a myc-Sema3A expression construct using the polyethyleneimine (PEI) method [27, 33]; for 20 μg DNA, 80 μg of PEI was used. The culture medium (DMEM-GlutaMax, supplemented with 2% fetal calf serum (FCS) and 1× PenStrep) was refreshed 1 day after transfection. Medium was collected 48 h after transfection and processed for Western Blot analysis as follows. Samples were spun to remove cell debris and boiled with loading buffer containing 10% SDS and 10% B-mercaptoethanol and loaded onto 8% SDS-PAGE gels. A standard curve of known protein concentrations (200 ng, 400 ng, 800 ng per well; hSema3A-Fc, R&D systems, 1250-S3) was loaded alongside the conditioned medium samples in order to determine the concentration of Sema3A or neuropilin in the conditioned medium. Membranes were blotted with rabbit-anti-Sema3A (1:1000, Abcam, Ab23393) or goat-anti-Fc (1:5000, Chemicon, AP113), developed using IRDye-secondary antibody (IRDye800® 1:2500, LI-COR Biosciences 925-32214) and scanned with the Odyssey infrared imaging system (LI-COR Biosciences). The resulting bands were analyzed for quantification purposes.

In preparation for immunocytochemistry, transfected cells were fixed with 4% paraformaldehyde (PFA) in 0.1 M phosphate buffer (pH 7.4) for 15 min, washed with PBS, and stained with the same antibodies as indicated above.

Dorsal Root Ganglion Explants Culture and Growth Cone Collapse Assay

Glass coverslips were pre-coated overnight with 0.5 mg/ml poly-ornithine (Sigma-Aldrich, P-3655). On the day of use,

the glass coverslips were washed with water and subsequently coated with 40 μg/ml laminin (Invitrogen). After a 2-h incubation at 37 °C, the laminin solution was removed, coverslips were washed briefly with DMEM/F12 medium, and freshly prepared culture medium (DMEM/F12 1:1 (GIBCO) containing N2 supplement (Sigma-Aldrich), 20 ng/ml NGF (Recombinant Rat beta-NGF, 556-NG-100, R&D Systems Europe, Ltd.), PenStrep (GIBCO), 2 mM L-glutamine (GIBCO)) was placed in each well before the DRG explants were added. A timed pregnant (E15) Wistar rat was deeply anesthetized by CO_2 inhalation and decapitated. The uterus was removed and placed into ice-cold Lebowitz (L15, GIBCO) medium. Under sterile conditions, embryos were removed from the uterus, and the spinal cord was dissected to reveal the dorsal root ganglia (DRGs). Individual DRGs (clean of any loose connective tissue and nerve roots) were centered on the laminin-coated glass coverslips, submerged in 500 μl of culture medium. DRG explants were cultured overnight at 37 °C with 5% CO_2 to allow for neurite outgrowth and growth cone formation.

Treatment solutions containing various quantities of GFP-, Sema3A-, and/or Npn-receptor body-conditioned medium were prepared by transfecting HEK cells with the appropriate expression plasmids and concentrating medium using an Amicon 100 kDa MWCO Ultra-15 device (Millipore). These samples were incubated on ice for 1 h to allow for stabilization of the protein interactions and were warmed briefly (in a water bath at 37 °C) before slowly applying the mixtures onto the DRGs. The volume added per well did not exceed 10% of the total volume in the well (maximum 50 μl treatment mixture in a well, containing 500 μl of culture medium). DRGs were incubated with conditioned medium samples for 30 min at 37oC. Following a 1-h fixation in 4%PFA/10% sucrose in PBS, DRGs were washed with PBS/0.2% Triton X (PBS/Tx) and subsequently incubated with Phalloidin-TRITC (Sigma, P1951) in PBS/Tx for 3 h at RT to visualize the actin cytoskeleton. Following a second wash in PBS/Tx, coverslips containing the DRGs were mounted onto glass slides using Mowiol 4–88 mounting medium (Sigma-Aldrich). Fluorescent images were obtained using a Zeiss Axiovert microscope, and growth cones were scored as normal (presence of lamellipodia and/or ≥ 3 filopodia) or collapsed (no lamellipodia, < 3 filopodia or bullet shaped) based on the classification described by [34]. For each treatment group, the percentage of growth cones was normalized to the percentage growth cones in the GFP condition. Data represents pooled data from DRGs across five independent experiments.

AAV Production

Npn1 is a co-receptor for Sema3A as well as for vascular endothelial growth factor (VEGF). We, therefore, generated AAV vectors encoding the extracellular domain of wild-type Npn1 (recognizing both Sema3A and VEGF) and AAV vectors which harbor Npn1 mutants recognizing either Sema3A (Npn1-Y297A-Fc; Herzog et al. 2011) or VEGF (Npn1-VEGF-Fc; 32). Based on the studies of Parker and colleagues [35, 36], an additional mutant (NPR1-T316R) was created in which the threonine (T) at position 316 to an arginine (R) results in a complete abolishment of VEGF-A164 binding (Npn1-T316R) and has significantly compromised Sema3A binding in biochemical assays [37], thus potentially generating a binding-deficient receptor.

Adeno-associated viral vector transfer plasmids containing the coding sequences for Npn1-Fc, Npn1-VEGF-Fc, Npn1-Y297A-Fc, Npn1-T316R, or Npn2-Fc (Moloney et al. submitted) were used to produce adeno-associated viral vectors (AAVs). The packaging plasmids containing cap and rep genes for serotype 8 (p5E18VD2/8) and the adenovirus helper functions (pAddeltaF6) were kindly provided by Jim Wilson (University of Pennsylvania, USA). A batch of AAV8 was made using the following protocol. Six 15-cm Petri dishes each containing 1.25×10^7 HEK 293T cells in Dulbecco's modified Eagle's medium (DMEM) containing 10% FCS and 1% penicillin/streptomycin (PS; all GIBCO) were prepared 1 day before transfection. The medium was refreshed 1 h prior to transfection to Iscoves modified Eagle medium (IMEM) containing 10% FCS, 1% PS, and 1% glutamine. Transfer plasmids were co-transfected using polyethyleneimine (PEI, MV25000; Polysciences Inc., Warrington, PA, USA) in a ratio of 1:1:1 with the plasmids resulting in a total amount of 50 μg of DNA per plate. The day after transfection, the medium was replaced with fresh IMEM with 10% FCS, 1% PS and 1% Glutamine. Two days later (3 days post-transfection), cells were harvested in D-phosphate buffered saline (D-PBS, GIBCO) and lysed with three freeze–thaw cycles. Genomic DNA was digested by adding 10 μg/ml DNAseI (Roche Diagnostics GmbH, Mannheim, Germany) into the lysate and incubating for 1 h at 37 °C. The crude lysate was cleared by ultracentrifugation at 4000 rpm for 30 min. The viral vector was purified from the crude lysate using the iodixanol gradient method [38–40], diluted in D-PBS/5% sucrose, and concentrated using an Amicon 100 kDa MWCO Ultra-15 device (Millipore). All AAV vectors were stored at − 80 °C until use. Titers (genomic copies/ml) were determined by quantitative PCR on viral DNA primers directed against the enhancer portion of the CMV promoter (forward: CCCACTTGGCAGTACATCAA; reverse: GGAAAGTC CCATAAGGTCATGT).

Intracortical Injections

Adult (>P90) rats were initially anesthetized with isoflurane (3%) and deeply anesthetized with an intraperitoneal injection of avertin (2,2,2-tribromoethanol, 20 μL/g). The animals were

placed in a stereotaxic frame, and the head was fixed with prilocaine (EMLA) covered earbars. Throughout the procedure, body temperature was monitored using a rectal probe and maintained at 37 °C with a homeothermic blanket (Harvard Apparatus Ltd., Edenbridge, Kent, UK) and a constant flow (1.5 L/min) of oxygen-enriched air was delivered to the animal's head. After local disinfection of the head with povidone–iodine, the scalp was cut with a scalpel and the skin flaps were retracted. The two sites of injection were in correspondence to the visual cortex, and their position was identified in respect to lambda (anterior 0 mm, lateral 3.8 mm; anterior 2 mm, lateral 3.8 mm).

A 1-mm burr hole was drilled through the skull at the two sites with a dental drill while continuously applying cold saline over the area to prevent overheating and consequent damage to the brain. A glass micropipette with a tip diameter of approximately 30 μm was filled with 0.75 μl of an AAV solution in sterile saline. When the meninges were exposed, the injections were delivered, by piercing the underlying dura mater via the glass micropipette connected to a syringe, at a depth of approximately 0.7 mm from the brain surface at each injection site. The injection was delivered at a rate of 0.5 μl/min with a 1-min interval before retracting the micropipette from the tissue. The scalp was then sutured with surgical suture. Animals were allowed to recover from anesthesia in a heated recovery box until fully conscious, and afterward, paracetamol (100 mg/kg) was administered in the water.

Visually Evoked Potentials

Adult (>P90) rats were anesthetized with an intraperitoneal injection of urethane (0.7 ml/hg; 20% solution in saline; Sigma) and head-fixed in a stereotaxic frame. After local disinfection of the head with povidone–iodine, the scalp was cut and a portion of the skull (4 × 4 mm) overlying the binocular visual cortex (binocular area Oc1B), contralateral to the deprived eye, was drilled, and removed, leaving the dura mater intact. The dura mater was then removed, a glass micropipette, filled with 3 M NaCl (2 MΩ impedance) was inserted at 3.5 to 3.8 mm lateral to lambda, and a subcutaneous ground electrode was placed in the cervical area. Throughout the procedure, body temperature was monitored using a rectal probe and maintained at 37 °C with a homeothermic blanket (Harvard Apparatus Ltd., Edenbridge, Kent, UK) and a constant flow (1.5 L/min) of oxygen-enriched air was delivered to the animal. Additional doses of urethane were used to keep the anesthesia level stable throughout the experiment. Visual stimuli were computer-generated horizontal sinusoidal gratings (0.08 cyc/deg) and were presented on a monitor suitably linearized by gamma correction and positioned centrally to the vertical midline. The stimulation consisted of the abrupt contrast reversal of sinusoidal gratings (temporal frequency 1 Hz). The receptive field of the recorded area was verified by stimulating the contralateral eye with a visual stimulus windowed to a vertical stripe in order to test the insertion of the electrode in the binocular area. Only traces responding to a windowed stimulus within a field of 20° from the vertical midline were considered.

Immunohistochemistry

Adult rats were transcardially perfused with cold phosphate buffer (0.1 M pH 7.4) and subsequently with cold paraformaldehyde 4% (in 0.1 M phosphate buffer pH 7.4). The brains were then collected and post-fixed by incubating them overnight at 4 °C in paraformaldehyde 4%. After incubation in EDTA (0.25 M in PBS, 48 h, 4 °C) and in sucrose (25% in PBS, 48 h, 4 °C), the brains were snap frozen in 2-methylbutane cooled to − 40 °C. The samples were embedded in Tissue-Tek O.C.T. (Sakura Finetek USA, Inc.) and 40-μm coronal sections were cut in a Leica cryostat and collected in Tris-buffered saline (TBS pH 7.4).

For Sema3A/NeuN double staining, free-floating sections were blocked by incubation in bovine serum albumin (BSA, 5%) and Triton X-100 (0.2%) in TBS for 1 h at room temperature (RT) and then incubated overnight at RT with Sema3A antibody (Santa Cruz C17, 1:50, BSA 5%, Triton X-100 0.2% in TBS) and for 2 h RT with Cy3-conjugated anti-Goat (AbCam ab6949, 1:500, BSA 5%, Triton X-100 0.2% in TBS) to complete the reaction. Afterwards, sections were counterstained with NeuN antibody (Merck Millipore MAB377, 1:500 BSA 5%, Triton X-100 0.2% in TBS) and for 2 h RT with Alexa Fluor 488-conjugated anti-Mouse (AbCam ab150105, 1:500, BSA 5%, Triton X-100 0.2% in TBS).

For each animal, at least 12 fields from 5 to 12 different coronal slices were acquired with a Zeiss Apotome.2 system with a Zeiss Plan-NEOFLUAR 20×, NA 0.5 lens. The primary visual cortex was identified by comparison with reference images [41]. All the images were centered on layer 4 of the cortex. We adjusted the imaging parameters to fit the brightest slice and never changed them throughout the entire experiment to ensure the same conditions for cell counting. NeuN-positive cells and Sema3A-positive nets were counted manually with the java plugin cell counter for ImageJ.

Experimental Design and Statistical Analysis

All statistical analysis has been performed in Prism (GraphPad, 5.0). A one-way ANOVA test was used, followed by Turkey's post-hoc test to compare multiple groups. Statistical significance was set at $p \leq 0.05$. When two groups were compared, we used an unpaired, two-tailed Student's t test. Normality of the data and homoscedasticity were controlled using SigmaStat. All data are presented as mean ± standard error of the mean (SEM).

Results

Sema3A Aggregation in Perineuronal Nets Correlates with Critical Period Closure

Previous work demonstrated that critical period closure was correlated with the formation in the visual cortex of WFA-positive PNNs [1, 14]. If Sema3A is involved in the inhibitory action of PNNs on OD plasticity, it could be expected that the accumulation of Sema3A in PNNs in the visual cortex correlates with critical period closure. To test this hypothesis, we performed WFA and Sema3A immunostaining at P14, P28, P45, and P90 (Fig. 1). Cells were considered to be positive when a full ring of staining surrounded a cell body. The results showed that Sema3A PNN-like staining was absent at P14 and P28, whereas Sema3A staining begins to be present at P45, in coincidence with the closure of the rat critical period for OD plasticity. Double staining with WFA and PV confirmed that Sema3A-positive structures were WFA-positive PNNs surrounding inhibitory PV-positive interneurons (Fig. 1). Thus, Sema3A-positive PNNs represent about half of the WFA-positive PNNs in the adult and increase in parallel with PNN formation during development.

To further corroborate the correlation between critical period closure, PNN formation, and the association of Sema3A with PNN, we dark-reared (DR) rats until adulthood (P90) and we assessed Sema3A staining in the visual cortex. DR is known to delay the closure of the critical period for OD as well as the formation of PNNs [1, 10]. Immunohistochemical staining for Sema3A showed that in DR rats, there was a significant reduction in the fraction of neurons (NeuN-positive cells) surrounded by Sema3A (Fig. 2a, b). In control animals, the average fraction of Sema3A-positive neurons was 3.6% (SEM = 0.78%, $N = 3$). Conversely, in dark-reared animals, this percentage significantly dropped to 1.6% (SEM = 0.37%, $N = 7$). This experiment allows to conclude that the persisting plasticity of DR rats is correlated with reduced levels of Sema3A-positive PNN structures. Taken together, these results indicate that the high levels of plasticity occurring during early developmental times or after DR are accompanied by a low density of Sema3A-positive PNN-structures in the visual cortex.

Soluble Npn Receptors, Except Npn1-VEGF-Fc, Are Able to Inhibit Sema3A-Induced Growth Cone Collapse

To test the role of Sema3A in PNN of adult rats, we developed a tool to interfere with Sema3A binding with its receptor in the adult visual cortex. Using the soluble neuropilin1 receptor fused to a human IgG Fc fragment supplied by Prof. Roman Giger (University of Michigan, USA), we performed site-directed mutagenesis to alter specific residues that had been shown to form the basis for selective Sema3A binding (Y297A mutation) (Npn1(Sema3A)-FC) [31]. We also adapted the "npn12ABC" mutant, created by Gu and colleagues [32], and the "Npn1-T316R-Fc" mutant [35, 36], by amplifying the ectodomain of these mutants and fusing it to a human IgG Fc fragment to create soluble receptors that bind respectively only VEGF, and potentially neither Sema3A nor VEGF. These constructs were inserted into adeno-associated viral plasmids under the control of the CMV promoter. The presence of the desired mutations was confirmed by sequencing. The Npn2-Fc construct was created by amplifying the ectodomain of the neuropilin2 gene and fusing it to a human IgG Fc fragment. Sequencing of the Npn1-Fc and the Npn2-Fc confirmed that the Npn portion is in frame with the Fc and that only one stop codon exists, positioned at the 3′end of the Fc portion. To characterize the expression of the soluble neuropilin receptors, HEK293T cells were transiently transfected with the different

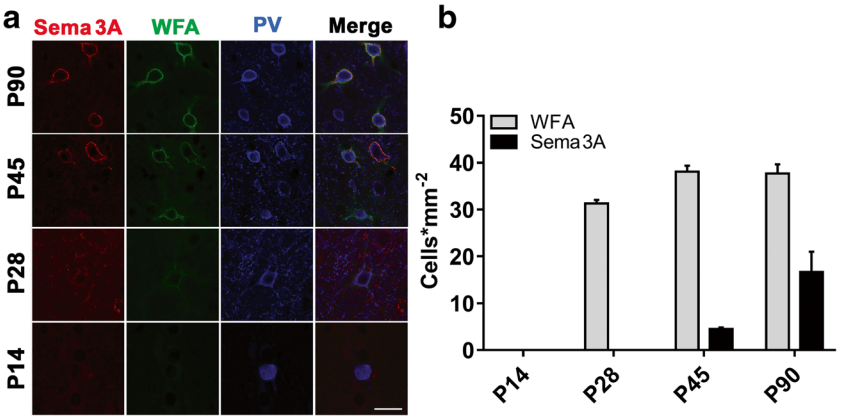

Fig. 1 Sema3A accumulates in PNN during late postnatal development. **a** Sections of the visual cortex of rats at different postnatal ages (P14, P28, P45, P90) were stained for Sema3A, WFA (to detect PNN) and PV (to identify parvalbumin-positive inhibitory interneurons). The right-hand column shows a merge of the Sema3A, WFA, and PV staining. Sema3A is not yet detectable in PNN at P28 but becomes increasingly visible in the cortex at P45 and P90. At P90 robust Sema-3A labeling is observed. Sema3A-positive PNNs are associated with PV cells. Scale bar 50 μm. **b** Quantification of the density of Sema3A-positive and WFA-positive cells in the visual cortex

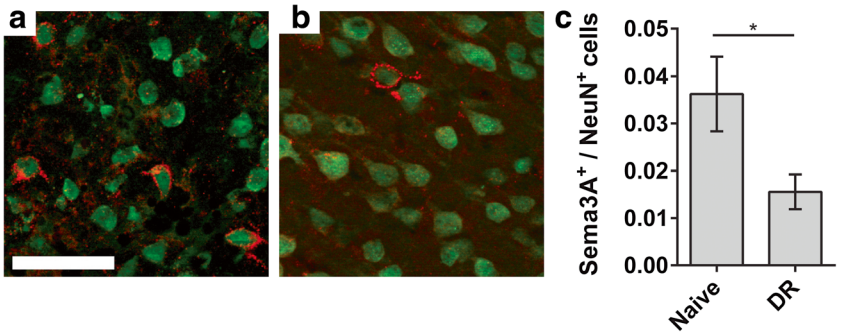

Fig. 2 Dark rearing prevents Sema3A aggregation in perineuronal nets. **a**, **b** Representative images of NeuN (green) and Sema3A (red) stained slices of the visual cortex in control ($N = 3$) and dark-reared ($N = 7$) rats respectively. **c** In dark-reared (DR) animals, fewer of the neurons are surrounded by an aggregation of Sema3A (*$p \leq 0.05$; two-tailed Student's T test)

Npn constructs. Immunocytochemistry was performed on cells 3 days post-transfection, and results indicate Npn1-Fc is expressed by the transfected cells, with a faint cloud of positive staining found outside the cells suggestive of secreted protein (Fig. 3a). The Npn1-Y297A-Fc and Npn1-T316R-Fc variants showed a similar cellular expression pattern as the Npn1-Fc (data not shown). Western blot analysis on conditioned medium harvested 3 days post-transfection showed that all soluble receptors are secreted into the medium and have the expected molecular weight (Fig. 3b).

The efficacy of soluble Npn receptors in counteracting Sema3A action was tested using the classical dorsal root ganglion (DRG) growth cone collapse assay. Explanted DRG neurons from an E15 rat embryo were cultured overnight on laminin in the presence of 20 ng/ml NGF. DRGs were treated for 30 min with GFP, Sema3A, and/or soluble Npn receptors, after which the explants were fixed and the cytoskeleton was visualized using Phalloidin-TRITC. The total number of collapsed growth cones (Fig. 3c) and intact growth cones (Fig. 3d) was manually counted and graphed to illustrate the percentage of total growth cones (Fig. 3e). Untreated and Npn-alone conditions did not differ from GFP condition. All conditions were normalized to the GFP treatment condition and represent pooled data from DRGs across five independent experiments.

Upon Sema3A treatment, approximately 44% growth cones remain ($p < 0.001$, compared to GFP treatment). The remaining gray bars illustrate the effects of pre-incubating Sema3A with the soluble Npn receptors (Fig. 3e). When Sema3A and Npn1-Fc are applied in combination, 60% growth cones remain after 30 min of treatment (Fig. 3e, $p < 0.01$, compared to Sema3A treatment alone). Npn1-Y297A-Fc, the isoform which is reported to selectively bind Sema3A and not VEGF, is also efficient in antagonizing Sema3A function with 68% of growth cones remaining intact in the presence of a 1:1 M ratio of Sema3A and Npn1-Y297A-Fc ($p < 0.001$, compared to Sema3A treatment alone). As expected, Npn1-VEGF-Fc, the isoform which should only bind VEGF, does not prevent Sema3A-induced collapse (50% growth cones, $p = 0.28$, ns compared to Sema3A treatment). Surprisingly, the Npn1-T316R-Fc variant also neutralized Sema3A function (71% growth cones in the presence of a 1:1 M ratio of Sema3A and Npn1-T316R-Fc, $p < 0.01$). The explanation for this may be that the T316R mutant was originally tested using a truncated Npn1 protein consisting only of the b1b2 and not the a1a2 domain [35]. It is plausible that the current Npn1-T316R-Fc variant, where the a1a2 domains are intact, "override" the effect of the T316R mutation, and allow the Npn1-T316R-Fc to continue binding of Sema3A. Since the Npn1-T316R-Fc is not a binding-neutral receptor body, we excluded this mutant from further in vivo study. Lastly, Npn2-Fc, a non-conventional Sema3A receptor [42, 43], is able to significantly inhibit Sema3A-induced growth cone collapse (56% growth cones, $p < 0.05$, compared to Sema3A treatment).

Neuropilin1-Fc Promotes Adult OD Plasticity in the Rat Visual Cortex

To functionally assess the role of Sema3A in the plasticity of the adult visual cortex, we tested whether the interference with Sema3A function, achieved by AAV8-mediated expression of Npn1-FC in the visual cortex, was sufficient to restore OD plasticity after 7 days of MD in adult (>P90) rats. We first assessed Npn1 expression in the injected rats using immunohistochemistry. As shown in Fig. 4a control sections showed low levels of expression of endogenous Npn1 in particular in layers II and V with some scattered faintly labeled cells in all other layers. The sections of the cortex injected with AAV8-Npn1-Fc shows numerous pyramidal neurons as well as other cells which express Npn1-Fc and diffuse extracellular staining of secreted Npn1-Fc covering the primary visual and extending to the neighboring cortical areas (Fig. 4b, c).

After assessing in vivo transduction and release of NPN1-Fc, we studied whether this treatment could affect Sema3A-positive PNNs. Thus, we transduced Npn1-FC into the visual cortex of adult rats and we labeled the sections for Sema3A and WFA. Since Npn1 is also a co-receptor for VEGF, as a

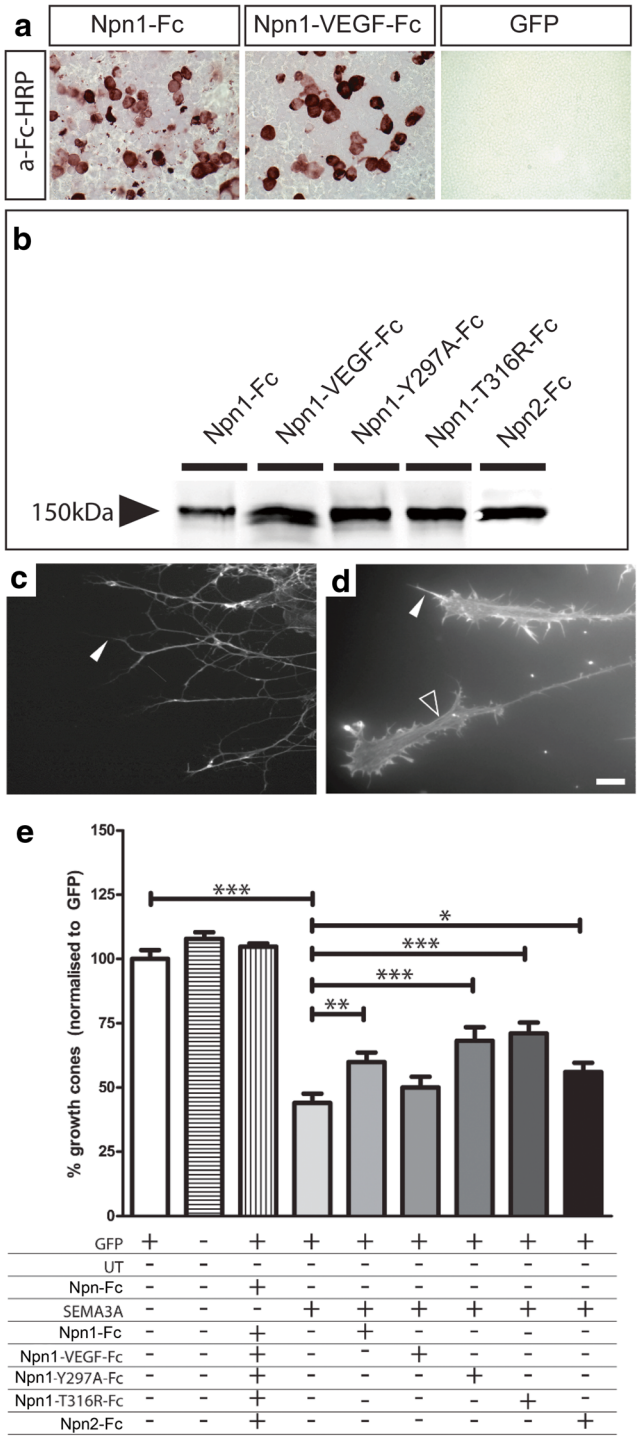

Fig. 3 Soluble neuropilin receptors are expressed and secreted from NRP-Fc transfected cells. **a** HEK293T cells were transiently transfected with Npn-Fc expression vectors and processed for immunocytochemistry using HRP-conjugated antibodies directed against Fc. Npn1-Fc and Npn1-VEGF-Fc are produced in the cell after transfection. **b** Medium samples were loaded onto 8% SDS-PAGE gels and blotted with anti-Fc. All soluble Npn receptors are secreted, detected by a band at 150 kDa. **c**–**e** Functional characterization of receptor bodies in the dorsal root ganglion (DRG) growth cone collapse assay. The growth cones E15 rat embryo DRG neurons collapse in the presence of Sema3A, the neurite tip contains no lamellipodia and ≤ 1 filopodium (**c**, arrowhead). **d** Application of a Sema3A and Npn1-Fc mix prevents Sema3A-induced collapse; the lamellipodia of the growth cones remains spread (open arrowhead) and ≥ 2 filopodia (filled arrowhead). **e** Quantification of growth cones after treatment with Sema3A and soluble Npn receptors. All conditions were normalized to GFP (open bar). Untreated (horizontally scored bar) and Npn-alone (vertically scored bar) conditions did not differ from GFP condition. Sema3A treatment (8.6 nM; light gray bar) results in a significant decrease in growth cones. The remaining five gray bars illustrate the effects of pre-incubating Sema3A with soluble Npn receptors. From left to right: upon combined Sema3A and Npn1-Fc treatment there is a significant increase in numbers of growth cones; Npn1-VEGF-Fc does not rescue Sema3A-induced growth cone collapse; Npn1-Y297A-Fc and Npn1-T316R show a similar and significant ability for neutralizing Sema3A function, and lastly, Npn2-Fc treatment significantly reverses Sema3A-induced growth cone collapse. Data were obtained from five independent experiments, error bars were generated using the SEM, and a Student's *t* test was used to determine significance (*$p < 0.05$, **$p < 0.01$, ***$p < 0.001$). Scale bar = 20 μm

control we transduced Npn1-VEGF-FC (AAV-VEGF group). This Npn-1 mutant isoform specifically interacts with VEGF [32] but not with Sema3A and does not interfere with Sema3A-induced growth cone collapse (Fig. 3e). Figure 4d, e shows that Sema3A-positive PNNs were not significantly affected by Sema3a inhibition, although a trend for a reduction was observed (AAV-Npn1 group $N = 5$, AAV-VEGF group $N = 5$, unpaired two-tailed Student's t test $p = 0.204$). This suggests that NPN1-Fc does not interrupt the association of Sema3A with PNN but rather interferes with Sema3A-mediated signaling.

We then assessed whether Sema3A inhibition could affect ocular dominance plasticity in the adult rat visual cortex. Figure 4f shows the ratios of the VEP amplitude obtained by stimulating the contralateral or the ipsilateral eye (C/I ratio) in non-deprived rats or after 1 week of monocular deprivation. In naive non-deprived rats, the C/I ratio was around 2 (binocular, BIN group; C/I ratio = 2.05 ± 0.06; $N = 5$; ANOVA $p < 0.0001$). Seven days of MD did not significantly change the C/I ratio (MD group, C/I ratio = 2.06 ± 0.15; $N = 4$. Post-hoc $p > 0.9$ vs Bin). Strikingly, the rats expressing Npn1-FC showed a significantly lower C/I ratio (AAV-Npn1 group; C/I ratio = 1.29 ± 0.08, $N = 4$. Post-hoc $p < 0.001$ vs BIN and MD) than BIN or MD rats indicating the activation of OD plasticity. As a control, rats were injected with an empty vector and monocularly deprived for 7 days (AAV-empty). These rats had a C/I ratio not different from untreated BIN or MD rats, and the C/I ratios were significantly higher than observed in AAV-Npn1 rats (C/I ratio = 1.87 ± 0.13, $N = 5$. Post-hoc $p > 0.8$ vs BIN, MD; $p < 0.01$ vs AAV-Npn1), showing that the injection procedure and the viral transduction did not alter plasticity levels. Since Npn1 is also a co-receptor for VEGF, we tested rats expressing Npn1-VEGF-FC (AAV-VEGF group) or Npn1-Y297A-FC

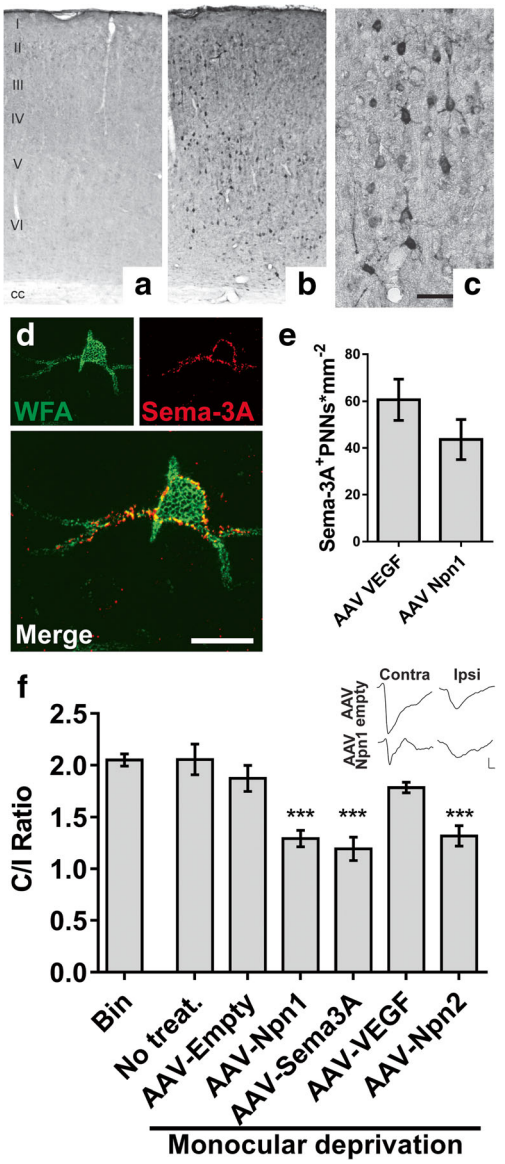

Fig. 4 AAV8 mediated NPN1-Fc expression in sections of the visual cortex of adult rat. **a** A section of a contralateral control hemisphere not injected with AAV8-NPN1-Fc. **b**, **c** Sections of the visual cortex injected with 1 μl of AAV8-NPN1-Fc 3 weeks after injection at low (**b**) and high magnifications (**c**). Sections were processed for immunohistochemistry for NPN1. The control sections show low levels of expression of endogenous NPN1 in particular in layer II and V with some faintly scattered cells in all other layers. The sections of the cortex injected with AAV8-NPN1-Fc shows numerous pyramidal neurons as well as other cells which express NPN1-Fc and diffuse extracellular staining of secreted NPN1-Fc. Representative sections are shown. cc is corpus callosum. Scale bar for panel B is 100 μm, for panel **c** is 25 μm. **d**, **e** The expression of Npn1 receptor body did not significantly alter the density of Sema3A, WFA double positive PNNs. **f** Contra/Ipsi ratio of AAV8 injected rats after 7 days of monocular deprivation. Examples of typical visual-evoked potential recordings are shown in the inset. The top and bottom rows represent respectively the contralateral and ipsilateral responses of an MD AAV-empty injected rat and of an MD AAV-Npn1 injected rat (scale bar 50 μV, 50 ms). The bars represent the ratio of the contralateral and ipsilateral VEPs amplitude in different treatment groups. No injection, transfection with an empty vector; a VEGF-specific version of Npn1-FC did not evoke any OD shift after 7 days of MD. Conversely, the transfection with Npr1-FC or with its Sema3A-specific version allowed for an OD shift, thus indicating the reactivation of adult OD plasticity. (***$p \leq 0.001$ vs no treatment and bin groups; one-way ANOVA; post-hoc: Turkey's multiple comparison test) (BIN $N = 5$; no treat $N = 4$; AAV-Npn1 $N = 4$; AAV-Empty $N = 5$; AAV-:Sema3A $N = 4$; AAV-:VEGF $N = 4$; AAV-Npn2 $N = 5$)

(AAV-Sema3A group), an NPN-1 mutant isoform specifically interacting with Sema3A [31] and functionally interfering with Sema3A induced growth cone collapse. While 7 days of MD did not significantly modify the C/I ratio in AAV-VEGF rats with respect to BIN, MD, and AAV-empty groups (C/I ratio = 1.78 ± 0.05, $N = 4$. Post-hoc $p > 0.5$ vs BIN, MD and AAV-empty, $p < 0.05$ vs AAV-Npn1, AAV-Sema3A); the receptor body specific for Sema3A elicited a plasticity-enhancing effect (C/I ratio = 1.19 ± 0.11, $N = 4$. Post-hoc $p < 0.01$ vs BIN, MD, and AAV-empty, $p < 0.05$ vs AAV-VEGF, $p > 0.9$ vs AAV-Npn1), mirroring the outcome of the injection of the neuropilin-1 receptor body.

We also tested another receptor body, Npn2-FC, which is based upon the isoform 2 of neuropilin. Remarkably, the injection with this construct, also allowed a shift in OD after 7 days of MD (C/I ratio = 1.32 ± 0.10, $N = 5$; Post-hoc $p < 0.01$ vs BIN, MD, and AAV-empty, $p < 0.05$ vs AAV-VEGF, $p > 0.9$ vs AAV-Npn1 and AAV-Sema3A), thus mimicking the effect of the previously tested isoform 1. Although the predominant class 3 semaphorin in PNN is Sema3A, Sema3B is also detectable in PNN (Vo et al. 2013). Sema3B is interacting with high affinity with Npn2, and the OD shift may, therefore, have been caused by functional interference with Sema3B. Alternatively, Npn2 can bind to Sema3A and functional interference with soluble Npn2 could also diminish Sema3A's function (Nasarre et al. 2009; Moloney et al., submitted).

Taken together, these results demonstrate that functional interference with the signaling of Sema3A can promote OD plasticity in adult rats and also corroborates the idea/notion that extracellular chemorepulsive molecules incorporated in the PNN could actively repress cortical plasticity in the adult brain and thus participate in the mechanisms for critical period closure.

Discussion

The role of PNNs in the plasticity of the adult visual cortex of rodents has repeatedly been investigated; however, little is known about the underlying molecular mechanisms by which PNN regulate plasticity. Our data demonstrate that Sema3A is a plasticity brake associated with PNNs in the rat adult visual cortex. Indeed, our results and previous data showed that Sema3A-positive PNNs in the visual cortex increase in parallel with critical period closure, whereas dark rearing, ChABC

treatment, or Crtl-1 deletion, interventions that preserve plasticity in visual cortical circuits, also reduce the accumulation of Sema3A-positive PNNs [29, 44]. These data suggest that Sema3A in PNNs can be actively modulated to facilitate or restrict plasticity.

To assess the functional role of Sema3A in adult OD plasticity, we developed and characterized a tool to antagonize Sema3A action in vivo. To selectively scavenge Sema3A, we prepared receptor bodies that were tested in the classical assay of DRG growth cone collapse and that could be delivered to the adult visual cortex by AAV vectors intracortical injection. We found that interfering with the function of Sema3A by expression of Npn1-Fc in the adult visual cortex promotes OD plasticity. Importantly, a plasticity-enhancing effect was also obtained following expression of a receptor body which selectively binds Sema3A and not VEGF. No effect was observed with the empty vector or a vector carrying a mutant isoform of Npn1 able to preferentially interact with VEGF but not Sema3A, strengthening the specificity of our results. These data mimic the enhancement in visual cortical plasticity observed after targeting PNNs by CSPG GAG digestion by means of chABC or by genetic deletion of the PNN stabilizing factors Crtl-1 and aggrecan both in rats and mice [1, 6, 8, 44, 45], suggesting that at least part of the action of PNNs on plasticity is mediated by Sema3A.

The active role of Sema3A in the adult visual cortex is also supported by the observation that two of its co-receptors, PlexinA1 and PlexinA4, are located on the plasma membrane of PNN-bearing PV cells constituting a microdomain closely associated with PNN bound Sema3A [29]. The ability of PV cells to respond to Sema3A-Plexin signaling is further supported by the abundance in PV cells of flotillin-1 [29], a lipid raft protein that is essential for Sema3A-induced growth cone turning and endocytosis [46]. It has to be underscored that all these actions of Sema3A located within PNNs can occur together with Sema3A independent actions of the PNN mediated by Plexin independent signaling pathways including protein-tyrosine phosphatase-sigma, leukocyte common-related phosphatase, or Nogo receptor-1 or receptor-3 [47–49].

The inhibitory action of Sema3A on OD plasticity could derive from a local effect on synaptic inputs onto PV cells as suggested by recent work on cerebellar and hippocampal circuits. These studies suggested that Sema3A in PNNs can be actively modulated to facilitate or restrict plasticity [13, 29, 50]. Once activated, semaphorin signaling has been shown to regulate the formation and function of synaptic contacts [51, 52]. Specifically, Sema3A increases the clustering of pre- and post-synaptic proteins in cortical neurons in vitro [53–56]. In the context of visual cortical plasticity, all these mechanisms could contribute to the experience-dependent selection of inputs onto PV cells, a cellular population that has been shown repeatedly to be involved in regulation of critical periods [15–22, 53]. In particular, it has been suggested that one of the early events of the plasticity process activated by monocular deprivation in juvenile mice is pruning of excitatory inputs onto PV cells that would lead to reduced inhibition and increased activation of cortical neurons by stimulation of the open eye. This mechanism would reduce with age, and its reactivation in the adult would enhance plasticity [23]. These experiments indicate that synaptic plasticity at the level of PV cells could be an upstream mechanism that could change the network properties of the visual cortical circuit [8, 16], modulating plasticity levels of the entire network. It is likely that PNN-bound molecules, such as Sema3A, act at this level to regulate plasticity levels in the adult visual cortex.

Intriguingly, a plasticity-enhancing activity was detected following expression of Npn2-Fc. It is not clear whether Npn2 is able to bind Sema3A: whereas early results showed the lack of Npn2 binding by Sema3A [57, 58] and persistence of Sema3A mediated repulsion in the presence of soluble Npn2 receptors [59], more recent data suggests that Npn2 can bind Sema3A and that blocking Npn2-Sema3A interaction abolish the chemorepulsive action of Sema3A [42]. These latter data were corroborated by the observation that soluble Npn2-Fc also inhibited Sema3A-induced growth cone collapse in vitro. It is possible that redundancy may exist between the two neuropilin receptors within the Sema3A pathway [43]. The potentiating effect of Npn2-FC on visual cortical plasticity could also be mediated by Sema3B, that is also present in PNNs [29], or other Npn2 binding factors, such as Sema3F, that have also been involved in plasticity [51, 53]. This observation raises the possibility that many different proteins are concentrated at the PNN by the interaction with CSPG GAGs. Recent work identified a basic motif composed of 15-amino acid enriched in arginine-lysine (RK) doublets at the N-terminal of Otx2 which is responsible for Otx2 binding to PNNs [6]. This peptide motif is present in a small number of proteins [6] that could potentially be enriched in the PNN. The C-terminus of Sema3A interacts with CSPGs [60], and the C-terminus of Sema3A contains an RK-peptide sequence which has very high homology to the Otx2 binding site. Moreover, Sema3A and Otx2 share the same preference for interaction with chondroitin sulfate E (CS-E) [6, 28]. Thus, Otx2, semaphorins, and other GAG-binding proteins could be concentrated by the PNN that could act as a molecular hub changing its function depending on its molecular composition. In this view, the regulation of PNN maturation and stability could represent a regulatory step to control the extracellular microenvironment surrounding PV cells and eventually plasticity of a brain circuit.

Acknowledgments The first four authors (marked with an asterisk) equally contributed to this study.

Funding Information This work was supported by the EU 7th Framework program (FP7) Marie Curie actions (AxRegen) 2008–2012 to JV.

Compliance with Ethical Standards

All experiments were carried out in accordance with the European Communities Council Directive of November 24, 1986 (86/609/EEC) and were approved by the Italian Ministry of Health (authorization number 1152/2016-PR).

References

1. Pizzorusso T, Medini P, Berardi N, Chierzi S, Fawcett JW, Maffei L (2002) Reactivation of ocular dominance plasticity in the adult visual cortex. Science 298:1248–1251
2. Härtig W, Brauer K, Brückner G (1992) Wisteria floribunda agglutinin-labelled nets surround parvalbumin-containing neurons. Neuroreport 3:869–872
3. Carulli D, Rhodes KE, Fawcett JW (2007) Upregulation of aggrecan, link protein 1, and hyaluronan synthases during formation of perineuronal nets in the rat cerebellum. J Comp Neurol 501:83–94
4. Bukalo O, Schachner M, Dityatev A (2001) Modification of extracellular matrix by enzymatic removal of chondroitin sulfate and by lack of tenascin-R differentially affects several forms of synaptic plasticity in the hippocampus. Neuroscience 104:359–369
5. Ye Q, Miao Q-L (2013) Experience-dependent development of perineuronal nets and chondroitin sulfate proteoglycan receptors in mouse visual cortex. Matrix Biol 32:352–363
6. Beurdeley M, Spatazza J, Lee HHC, Sugiyama S, Bernard C, Di Nardo AA et al (2012) Otx2 binding to perineuronal nets persistently regulates plasticity in the mature visual cortex. J Neurosci 32:9429–9437
7. Gogolla N, Caroni P, Luthi A, Herry C (2009) Perineuronal nets protect fear memories from erasure. Science 325:1258–1261
8. Lensjø KK, Lepperød ME, Dick G, Hafting T, Fyhn M (2017) Removal of perineuronal nets unlocks juvenile plasticity through network mechanisms of decreased inhibition and increased gamma activity. J Neurosci 37:1269–1283
9. Pizzorusso T, Medini P, Landi S, Baldini S, Berardi N, Maffei L (2006) Structural and functional recovery from early monocular deprivation in adult rats. Proc Natl Acad Sci U S A 103:8517–8522
10. Sur M, Frost DO, Hockfield S (1988) Expression of a surface-associated antigen on Y-cells in the cat lateral geniculate nucleus is regulated by visual experience. J Neurosci 8:874–882
11. Guimarães A, Zaremba S, Hockfield S (1990) Molecular and morphological changes in the cat lateral geniculate nucleus and visual cortex induced by visual deprivation are revealed by monoclonal antibodies Cat-304 and Cat-301. J Neurosci 10:3014–3024
12. Sale A, Maya Vetencourt JF, Medini P, Cenni MC, Baroncelli L, De Pasquale R et al (2007) Environmental enrichment in adulthood promotes amblyopia recovery through a reduction of intracortical inhibition. Nat Neurosci 10:679–681
13. de Winter F, Kwok JCF, Fawcett JW, Vo TT, Carulli D, Verhaagen J (2016) The chemorepulsive protein semaphorin 3A and perineuronal net-mediated plasticity. Neural Plast 2016:3679545
14. Lensjø KK, Christensen AC, Tennøe S, Fyhn M, Hafting T (2017) Differential expression and cell-type specificity of perineuronal nets in hippocampus, medial entorhinal cortex, and visual cortex examined in the rat and mouse. eNeuro 4:ENEURO.0379–ENEU16.2017. https://doi.org/10.1523/ENEURO.0379-16.2017
15. Gu Y, Tran T, Murase S, Borrell A, Kirkwood A, Quinlan EM (2016) Neuregulin-dependent regulation of fast-spiking interneuron excitability controls the timing of the critical period. J Neurosci 36:10285–10295
16. Miao Q, Yao L, Rasch MJ, Ye Q, Li X, Zhang X (2016) Selective maturation of temporal dynamics of Intracortical excitatory transmission at the critical period onset. Cell Rep 16:1677–1689
17. He L-J, Liu N, Cheng T-L, Chen X-J, Li Y-D, Shu Y-S, Qiu ZL, Zhang XH (2014) Conditional deletion of Mecp2 in parvalbumin-expressing GABAergic cells results in the absence of critical period plasticity. Nat Commun 5:5036
18. Sun Y, Ikrar T, Davis MF, Gong N, Zheng X, Luo ZD, Lai C, Mei L et al (2016) Neuregulin-1/ErbB4 signaling regulates visual cortical plasticity. Neuron 92:160–173
19. Tang Y, Stryker MP, Alvarez-Buylla A, Espinosa JS (2014) Cortical plasticity induced by transplantation of embryonic somatostatin or parvalbumin interneurons. Proc Natl Acad Sci U S A 111:18339–18344
20. Morishita H, Cabungcal J-H, Chen Y, Do KQ, Hensch TK (2015) Prolonged period of cortical plasticity upon redox dysregulation in fast-spiking interneurons. Biol Psychiatry 78:396–402
21. Kobayashi Y, Ye Z, Hensch TK (2015) Clock genes control cortical critical period timing. Neuron 86:264–275
22. Hensch TK (2005) Critical period plasticity in local cortical circuits. Nat Rev Neurosci 6:877–888
23. Kuhlman SJ, Olivas ND, Tring E, Ikrar T, Xu X, Trachtenberg JT (2013) A disinhibitory microcircuit initiates critical-period plasticity in the visual cortex. Nature 501:543–546
24. Wang D, Fawcett J (2012) The perineuronal net and the control of CNS plasticity. Cell Tissue Res 349:147–160
25. Despras G, Bernard C, Perrot A, Cattiaux L, Prochiantz A, Lortat-Jacob H, Mallet JM (2013) Toward libraries of biotinylated chondroitin sulfate analogues: from synthesis to in vivo studies. Chemistry 19:531–540
26. Cardin AD, Weintraub HJ (1989) Molecular modeling of protein-glycosaminoglycan interactions. Arteriosclerosis 9:21–32
27. De Wit J, De Winter F, Klooster J, Verhaagen J (2005) Semaphorin 3A displays a punctate distribution on the surface of neuronal cells and interacts with proteoglycans in the extracellular matrix. Mol Cell Neurosci 29:40–55
28. Dick G, Tan CL, Alves JN, Ehlert EME, Miller GM, Hsieh-Wilson LC, Sugahara K, Oosterhof A et al (2013) Semaphorin 3A binds to the perineuronal nets via chondroitin sulfate type E motifs in rodent brains. J Biol Chem 288:27384–27395
29. Vo T, Carulli D, Ehlert EME, Kwok JCF, Dick G, Mecollari V, Moloney EB, Neufeld G et al (2013) The chemorepulsive axon guidance protein semaphorin3A is a constituent of perineuronal nets in the adult rodent brain. Mol Cell Neurosci 56:186–200
30. Conrad AH, Zhang Y, Tasheva ES, Conrad GW (2010) Proteomic analysis of potential keratan sulfate, chondroitin sulfate A, and hyaluronic acid molecular interactions. Invest Ophthalmol Vis Sci 51:4500–4515
31. Herzog B, Pellet-Many C, Britton G, Hartzoulakis B, Zachary IC (2011) VEGF binding to NRP1 is essential for VEGF stimulation of endothelial cell migration, complex formation between NRP1 and VEGFR2, and signaling via FAK Tyr407 phosphorylation. Mol Biol Cell 22:2766–2776
32. Gu C, Limberg BJ, Whitaker GB, Perman B, Leahy DJ, Rosenbaum JS, Ginty DD, Kolodkin AL (2002) Characterization of neuropilin-1 structural features that confer binding to

semaphorin 3A and vascular endothelial growth factor 165. J Biol Chem 277:18069–18076
33. Reed SE, Staley EM, Mayginnes JP, Pintel DJ, Tullis GE (2006) Transfection of mammalian cells using linear polyethylenimine is a simple and effective means of producing recombinant adeno-associated virus vectors. J Virol Methods 138:85–98
34. Kapfhammer JP, Xu H, Raper JA (2007) The detection and quantification of growth cone collapsing activities. Nat Protoc 2:2005–2011
35. Parker MW, Xu P, Li X, Vander Kooi CW (2012) Structural basis for selective vascular endothelial growth factor-A (VEGF-A) binding to neuropilin-1. J Biol Chem 287:11082–11089
36. Parker MW, Hellman LM, Xu P, Fried MG, Vander Kooi CW (2010) Furin processing of semaphorin 3F determines its anti-angiogenic activity by regulating direct binding and competition for neuropilin. Biochemistry 49:4068–4075
37. Parker MW, Vander Kooi CW (2017) Plate-based assay for measuring direct semaphorin-neuropilin interactions. Methods Mol Biol 1493:73–87
38. Hermens WT, ter Brake O, Dijkhuizen PA, Sonnemans MA, Grimm D, Kleinschmidt JA et al (1999) Purification of recombinant adeno-associated virus by iodixanol gradient ultracentrifugation allows rapid and reproducible preparation of vector stocks for gene transfer in the nervous system. Hum Gene Ther 10:1885–1891
39. Zolotukhin S, Byrne BJ, Mason E, Zolotukhin I, Potter M, Chesnut K, Summerford C, Samulski RJ et al (1999) Recombinant adeno-associated virus purification using novel methods improves infectious titer and yield. Gene Ther 6:973–985
40. Verhaagen J, Hobo B, Ehlert EME, Eggers R, Korecka JA, Hoyng SA et al (2018) Small scale production of recombinant adeno-associated viral vectors for gene delivery to the nervous system. Methods Mol Biol 1715:3–17
41. Paxinos G, Franklin KBJ (2004) The mouse brain in stereotaxic coordinates. Gulf Professional Publishing
42. Nasarre C, Koncina E, Labourdette G, Cremel G, Roussel G, Aunis D, Bagnard D (2009) Neuropilin-2 acts as a modulator of Sema3A-dependent glioma cell migration. Cell Adhes Migr 3:383–389
43. Cariboni A, Davidson K, Rakic S, Maggi R, Parnavelas JG, Ruhrberg C (2011) Defective gonadotropin-releasing hormone neuron migration in mice lacking SEMA3A signalling through NRP1 and NRP2: implications for the aetiology of hypogonadotropic hypogonadism. Hum Mol Genet 20:336–344
44. Carulli D, Pizzorusso T, Kwok JCF, Putignano E, Poli A, Forostyak S, Andrews MR, Deepa SS et al (2010) Animals lacking link protein have attenuated perineuronal nets and persistent plasticity. Brain 133:2331–2347
45. Rowlands D, Lensjø KK, Dinh T, Yang S, Andrews MR, Hafting T, Fyhn M, Fawcett JW et al (2018) Aggrecan directs extracellular matrix-mediated neuronal plasticity. J Neurosci 38:10102–10113
46. Carcea I, Ma'ayan A, Mesias R, Sepulveda B, Salton SR, Benson DL (2010) Flotillin-mediated endocytic events dictate cell type-specific responses to semaphorin 3A. J Neurosci 30:15317–15329
47. Shen Y, Tenney AP, Busch SA, Horn KP, Cuascut FX, Liu K, He Z, Silver J et al (2009) PTPsigma is a receptor for chondroitin sulfate proteoglycan, an inhibitor of neural regeneration. Science 326:592–596
48. Fisher D, Xing B, Dill J, Li H, Hoang HH, Zhao Z, Yang XL, Bachoo R et al (2011) Leukocyte common antigen-related phosphatase is a functional receptor for chondroitin sulfate proteoglycan axon growth inhibitors. J Neurosci 31:14051–14066
49. Dickendesher TL, Baldwin KT, Mironova YA, Koriyama Y, Raiker SJ, Askew KL, Wood A, Geoffroy CG et al (2012) NgR1 and NgR3 are receptors for chondroitin sulfate proteoglycans. Nat Neurosci 15:703–712
50. Carulli D, Foscarin S, Faralli A, Pajaj E, Rossi F (2013) Modulation of semaphorin3A in perineuronal nets during structural plasticity in the adult cerebellum. Mol Cell Neurosci 57:10–22
51. Wang Q, Chiu S-L, Koropouli E, Hong I, Mitchell S, Easwaran TP, Hamilton NR, Gustina AS et al (2017) Neuropilin-2/PlexinA3 receptors associate with GluA1 and mediate Sema3F-dependent homeostatic scaling in cortical neurons. Neuron 96:1084–1098.e7
52. Orr BO, Fetter RD, Davis GW (2017) Retrograde semaphorin-plexin signalling drives homeostatic synaptic plasticity. Nature 550:109–113
53. Tran TS, Rubio ME, Clem RL, Johnson D, Case L, Tessier-Lavigne M, Huganir RL, Ginty DD et al (2009) Secreted semaphorins control spine distribution and morphogenesis in the postnatal CNS. Nature 462:1065–1069
54. Uesaka N, Uchigashima M, Mikuni T, Nakazawa T, Nakao H, Hirai H, Aiba A, Watanabe M et al (2014) Retrograde semaphorin signaling regulates synapse elimination in the developing mouse brain. Science 344:1020–1023
55. Sahay A, Kim C-H, Sepkuty JP, Cho E, Huganir RL, Ginty DD et al (2005) Secreted semaphorins modulate synaptic transmission in the adult hippocampus. J Neurosci 25:3613–3620
56. Bouzioukh F, Daoudal G, Falk J, Debanne D, Rougon G, Castellani V (2006) Semaphorin3A regulates synaptic function of differentiated hippocampal neurons. Eur J Neurosci 23:2247–2254
57. Chen H, Chédotal A, He Z, Goodman CS, Tessier-Lavigne M (1997) Neuropilin-2, a novel member of the neuropilin family, is a high affinity receptor for the semaphorins Sema E and Sema IV but not Sema III. Neuron 19:547–559
58. Takahashi T, Nakamura F, Jin Z, Kalb RG, Strittmatter SM (1998) Semaphorins A and E act as antagonists of neuropilin-1 and agonists of neuropilin-2 receptors. Nat Neurosci 1:487–493
59. Chen H, He Z, Bagri A, Tessier-Lavigne M (1998) Semaphorin–neuropilin interactions underlying sympathetic axon responses to class III semaphorins. Neuron 21:1283–1290
60. Corredor M, Bonet R, Moure A, Domingo C, Bujons J, Alfonso I, Pérez Y, Messeguer À (2016) Cationic peptides and peptidomimetics bind glycosaminoglycans as potential Sema3A pathway inhibitors. Biophys J 110:1291–1303